



Near-infrared intraoperative molecular imaging with conventional neurosurgical microscope can be improved with narrow band “boost” excitation

Carrie Li^{1,2} · Love Buch² · Steve Cho^{1,2} · John Y. K. Lee²

Received: 18 February 2019 / Accepted: 26 August 2019 / Published online: 3 September 2019
© Springer-Verlag GmbH Austria, part of Springer Nature 2019

Abstract

Background Intraoperative visualization of brain tumors with near-infrared (NIR)-fluorescent dyes is an emerging method for tumor margin approximation but are limited by existing fluorescence detection platforms. We previously showed that a dedicated NIR imaging platform outperformed a state-of-the-art neurosurgical microscope in fluorescence signal characteristics. This study examined whether conventional neurosurgical microscope NIR signal could be improved with the addition of a narrow wavelength excitation source.

Methods Imaging was conducted with a broad-spectrum neurosurgical microscope and commercial near-infrared module. Addition of an 805-nm laser was used to “boost” NIR excitation of indocyanine green (ICG). In vitro quantification was performed on serial dilutions of ICG. Patients underwent tumor resection with delayed 24-h imaging of ICG infusion. NIR fluorescence of dura, cortex, or tumor was quantified from images prior to (pre-boost) and following added excitation with the laser (post-boost). Signal to background ratio (SBR) of pre- and post-boost was calculated as a readout of image enhancement.

Results In vitro, excitation boost effected a 29% increase in mean SBR in six serial dilutions of ICG. Intraoperative boost was performed in 11 patients including meningioma, glioblastoma multiforme, and metastases. Increase in tumor fluorescence was pronounced under direct tumor visualization. Across all patients, boost excitation resulted in 35% mean improvement from pre-boost SBR ($p < 0.001$).

Conclusion Neurosurgical microscopes remain the preferred method of visualizing tumor during intracranial surgery. However, current modalities for NIR signal detection are suboptimal. We demonstrate that augmentation of a fluorescence microscope module with a focused excitation source is a simple mechanism of improving NIR tumor visualization.

Clinical trial registration [NCT03262636](https://clinicaltrials.gov/ct2/show/study/NCT03262636)

Keywords Near-infrared (NIR) · Indocyanine green (ICG) · Fluorescence · Intraoperative molecular imaging · Tumor

This article is part of the Topical Collection on *Brain Tumors*

Presentations • Digital Poster Presentation: Pennsylvania Neurosurgical Society’s (PNS) 105th Scientific Meeting, July 21, 2018 in Hershey, Pennsylvania

✉ Carrie Li
carrie.li@pennmedicine.upenn.edu

¹ Perelman School of Medicine University of Pennsylvania, 3400 Spruce St, Philadelphia, PA, USA

² Department of Neurosurgery, Hospital of the University of Pennsylvania, 3400 Spruce St, Philadelphia, PA 19104, USA

Introduction

Intraoperative visualization of brain tumors with fluorescent dyes is an emerging method for real-time identification of tumor and with potential to delineate surgical margins. Near-infrared (NIR)-fluorescent dyes demonstrate superior tissue penetration and sensitivity compared to visible-light fluorescence with dyes such as 5-ALA and sodium fluorescein [3]. For these reasons, our group has pioneered use of NIR fluorophore indocyanine green (ICG), an FDA-approved vascular imaging perfusion agent, for intraoperative visualization of various intracranial tumors [5–7]. We have further demonstrated a technique termed Second Window ICG (SWIG), in which infusion of high-dose ICG approximately 24 h prior to surgery results in preferential accumulation of residual dye in

tumor tissue relative to surrounding vasculature and normal brain parenchyma [10].

Neurosurgical microscopes are the workhorse for surgical resection, and the addition of a near-infrared module to a pre-existing neurosurgical microscope is the primary means of filtering emissions in the NIR spectrum. A recent publication by our group comparing sensitivity and range of detection between two imaging modalities demonstrated that a commercial NIR-imaging platform outperformed a state-of-the-art neurosurgical microscope in dynamic range and overall fluorescence compared to background tissue [1]. However, neurosurgery workflow generally requires use of the microscope with its optimized illumination, magnification, and intuitive ergonomics for surgery. This study explored a simple method of improving neurosurgical microscope visualization of tumor when using Second Window ICG.

We hypothesized that a narrow wavelength excitation source could be applied to a pre-existing neurosurgical microscope to improve detection of NIR fluorescence. This simple modification, which we have termed a narrow-window “boost” excitation, underscores the necessity for fluorescence modules employing high power, narrow frequency excitation to enhance fluorescence visualization. Future microscope-integrated fluorescent modules incorporating dye-specific excitation sources offer potential to eliminate intermediate logistics of separate microscope and camera interfaces and greatly enhance the surgeon’s operative workflow.

Methods

In vitro and intraoperative NIR detection was performed utilizing the near-infrared FL800™ module of the commercially available Leica OH6 (Leica Microsystems, Buffalo Grove, IL) surgical microscope. The Leica OH6 light source is a 300- to 400-watt xenon lamp which produces broadband emissions in the visible and NIR spectrum. The default illumination filter (Filter 1) for standard white light visualization spans 400–720 nm and thus blocks the near-infrared and infrared spectral regions. In contrast, the FL800™ utilizes a filter (Filter 2) which ranges from 400 nm to approximately 805 nm (400–805 nm), the upper bound corresponding to the excitation wavelength of ICG. Resultant near-infrared emission is passed through a 800–880-nm filter which allows for capture of NIR peak excitation at 835 nm. The NIR camera is a 1/2 in. CCD Sony XCE150 monochrome with pixel resolution of $752 \times 582 = 0.5$ megapixel resolution capable of 50 Hz frequency recording.

“Boost” excitation was achieved by positioning a commercially available NIR camera system (VisionSense Iridium™, Philadelphia, PA) adjacent to the Leica OH6 with orientation of its 805-nm laser (11 mW/cm² at 300-mm working distance) excitation source incident upon region of interest (Fig. 1). This



Fig. 1 Illustration of intraoperative boost set-up. This cartoon rendering depicts how narrow-window “boost” excitation was achieved by positioning of a commercially available VisionSense NIR camera system (right) adjacent to the Leica OH6 (center) with orientation of its mobile 805-nm laser excitation source incident upon region of interest. The Leica OH6 FL800 near-infrared module projects collected fluorescent signal in black/white on an attached monitor display (not shown). Activation of the VisionSense laser in addition to the modified Leica OH6 xenon light source results in visible enhancement of fluorescent signal

boost was applied in addition to the modified Leica OH6 xenon light source (300 W) employing Filter 2. All images were acquired under conditions of minimized ambient light to enhance detection of tumor-specific NIR fluorescence.

In vitro measurement of indocyanine green (Akorn Pharmaceuticals, Decatur, IL) fluorescence intensity was performed as previously described via preparation of six twofold serial dilutions of ICG (2.58–82.6 μM) in a 96-well plate [1]. All measurements were obtained from a working distance of 30 cm with the VisionSense laser positioned approximately 35 cm from the region of interest. Comparison of excitation modalities was additionally performed in eleven patients undergoing resection of intracranial tumors with SWIG as part of an ongoing IRB-approved protocol. In 2014, a prospective study was initiated with an enrollment goal of 350 patients (study details with full inclusion and exclusion criterion can be found under NCT03262636 at clinicaltrials.gov). Informed consent was obtained for all patients. Off-label infusion of either 2.5 or 5.0 mg/kg ICG was performed approximately 24 h prior to anesthetic induction (Table 1). Decision to image dura, cortex, or tumor was made at the discretion of attending surgeon, at which point NIR boosts were applied in the manner outlined above. There were no postoperative complications or adverse reactions at the time of or immediately following ICG administration.

For all cases, NIR fluorescence was recorded in .mp4 format in simultaneous visible and NIR black/white. Videos were analyzed at timepoints at which boosts were applied. Change in observed fluorescence intensity was calculated from images obtained immediately prior to and immediately after boost

Table 1 Patient tumor characteristics

	Patient ID	Sex	Age (year)	Tumor type	Tumor side	Tumor location	ICG dose (mg/kg)
1	ICG 186	F	52	Meningioma WHO I	R (approach)*	Pineal	5
2	ICG 189	F	64	Meningioma WHO I	L	Sphenoidal	5
3	ICG 206	M	70	Meningioma WHO I	L	Parietal	5
4	ICG 210	M	76	Meningioma WHO I	R (approach)	Middle fossa	5
5	ICG 179	M	37	Meningioma WHO II	L	Falcine convexity	5
6	ICG 181	F	71	Glioblastoma WHO IV, IDH1-wild type	R	Fronto-temporal	5
7	ICG 220	M	67	Glioblastoma WHO IV, IDH1-wild type	L	Temporal	2.5
8	ICG 185	F	44	Metastatic melanoma	L	Temporal	5
9	ICG 191	M	73	Metastatic melanoma	L	Frontal	5
10	ICG 222	M	64	Metastatic melanoma	L	Frontal	2.5
11	ICG 184	F	47	Metastatic breast carcinoma	R	Frontal	5

*Cases for which there was no laterality of the lesion are classified by side of surgical approach

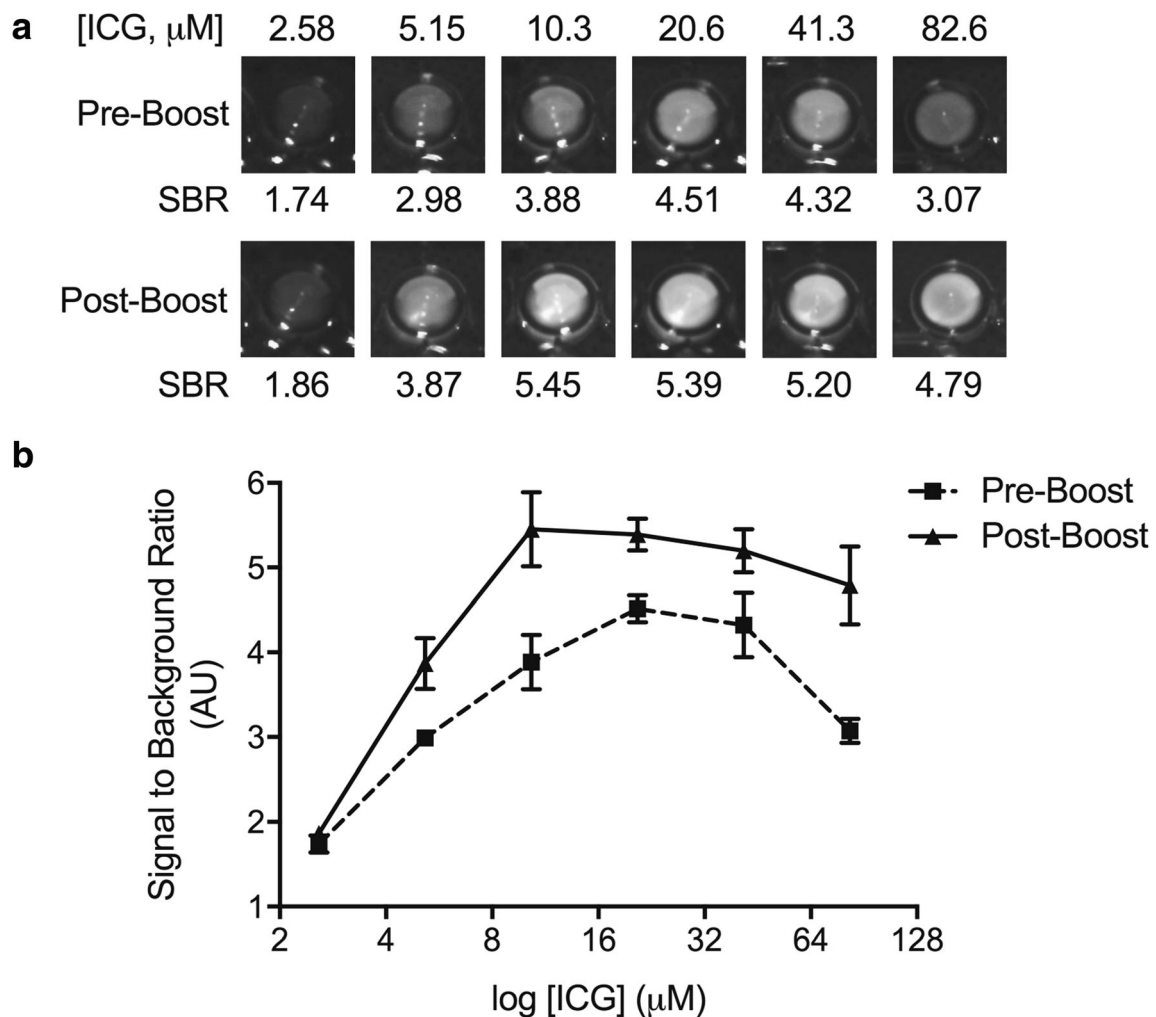


Fig. 2 Excitation boost of ICG serial dilution in vitro. **a** Twofold serial dilutions of ICG were imaged with the near-infrared FL800™ fluorescence module of the Leica OH6 surgical microscope (pre-boost, top row) and following addition of a focused 805-nm laser source (post-boost, bottom row). Corresponding ICG concentrations (range 2.58–

82.6 μM) and signal to background ratios (SBR) are provided. **b** Plot of SBR measurements pre-boost versus post-boost as a function of log concentration of ICG (μM). Increase in SBR post-boost was determined to be statistically significant by two-tailed ratio paired *t* test ($p = 0.007$)

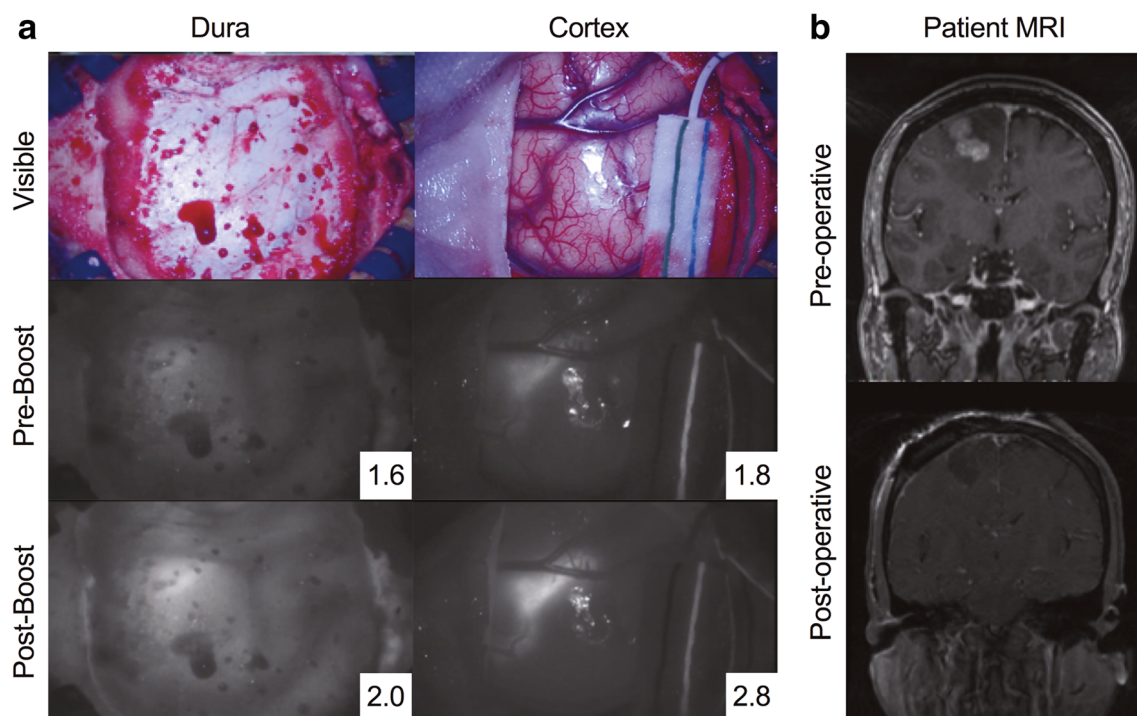


Fig. 3 Example NIR boost in a patient (ICG 184) with metastatic breast carcinoma. **a** Representative intraoperative views of SWIG-guided resections as viewed through visible light (upper panel) or black and white NIR fluorescence pre-boost (middle panel) and post-boost (lower

panel). **b** Preoperative (upper panel) and postoperative (lower panel) coronal MRI images demonstrating resection of enhancing lesions in the right frontal lobe

timepoints using ImageJ software (<https://imagej.nih.gov>). Corresponding signal to background ratio (SBR) for each case was calculated as the mean of pixel intensity at 5 points of interest sampled in a circumferential fashion within the area of fluorescent tumor relative to normal tissue [1]. Difference in mean pre- and post-boost SBR were reported as relative percent increase (%). Error was calculated as standard deviation from mean SBR, and comparison of mean difference in pre- vs. post-boost SBR was conducted by both a Wilcoxon matched-pairs signed rank test and a two-tailed ratio paired *t* test using the GraphPad Prism version 7.00 for Mac OS X, GraphPad Software, La Jolla California USA, (<https://www.graphpad.com>).

Results

In vitro comparison of NIR excitation boost

To assess the extent of NIR excitation boost, fluorescence images were acquired with six samples of twofold serial dilutions of ICG (2.58–82.6 μM), first under illumination by the xenon light source (Filter 2, pre-boost) and subsequently under the VisionSense 805-nm laser source (post-boost). A visible increase in fluorescence intensity was observed across all concentrations as a result of excitation boost (Fig. 2a). Using the standard neurosurgical microscope, signal to background (SBR) ranged from 1.74 ± 0.10 to 4.51 ± 0.16 . Application of the

805-nm laser resulted in a significant increase in SBR ranging from 1.86 ± 0.09 to 5.45 ± 0.43 (two-tailed ratio paired Student's *t* test, $p = 0.007$) (Fig. 2b). Overall mean enhancement of SBR was $29\% \pm 17\%$ across all concentrations of ICG with a maximum SBR boost of 56.0% corresponding to 82.6 μM .

Maximal pre-boost SBR (4.51) was observed at 20.6 μM and exhibited a decline in fluorescence at 41.3 μM and 82.6 μM , consistent with previous observations of auto-quenching of ICG fluorescence at higher concentrations [1]. Maximal post-boost SBR (5.45) was achieved at 10.3 μM and maintained at a relatively similar level with increasing ICG concentration. These results suggest that boost excitation offers significant enhancement of fluorescence across a broad range of ICG concentrations.

Comparative assessment of intraoperative NIR excitation boost

Eleven patients who underwent SWIG-guided tumor resection with NIR excitation boost as part of an ongoing clinical trial were included in the analysis. The median age of study subjects was 64 years. (range 37 to 76 years) with 6 males and 5 females. Final pathologies comprised meningioma (5), glioblastoma multiforme (2), metastatic breast cancer (1), and metastatic melanoma (3) (Table 1).

Intraoperative boost excitation was performed on 4 patients prior to tumor exposure. Representative intraoperative images

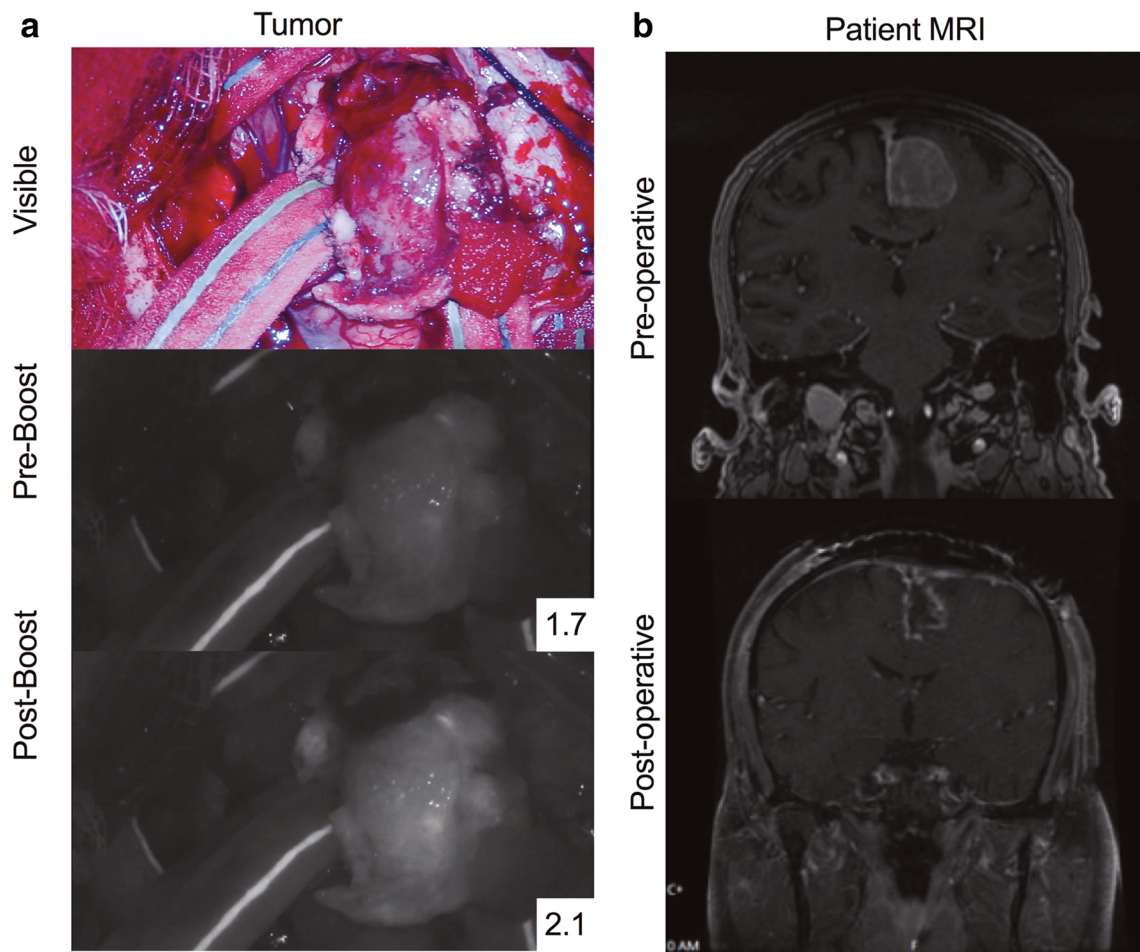


Fig. 4 Example NIR boost in a patient (ICG 179) with meningioma, WHO II. **a** Intraoperative tumor views of an atypical meningioma seen under visible white light (upper panel) or near-infrared fluorescence (middle and lower panels). Boost excitation produced significant

increase in tumor fluorescence with change SBR 1.7 ± 0.24 to 2.1 ± 0.48 . **b** Coronal MRI of parasagittal meningioma pre- (upper panel) and post- (lower panel) resection with SWIG

of dura and cortex in a patient with brain metastasis (ICG 184) are shown in Fig. 3a. Tumor was not visible to the surgeon under white light at the level of both dura and cortex (Fig. 3a, upper panel). NIR visualization using the Leica OH6 FL800™ module alone (pre-boost) revealed ICG accumulation in the right frontal lobe from the superior aspect with an SBR of 1.6 ± 0.21 (Fig. 3a, middle panel). Excitation with the VisionSense laser (post-boost) increased the dura view SBR to 2.0 ± 0.32 . Meanwhile, a cortex view of the same patient yielded a strong gain in NIR signal post-boost with an SBR of 2.8 ± 0.36 from 1.8 ± 0.18 (pre-boost) (Fig. 3a, lower panel). Moreover, ICG accumulation seen from the level of dura and cortex was concordant with tumor location as determined by preoperative MRI (Fig. 3b). These results demonstrate an effective enhancement of tumor visualization with excitation boost both prior to and following dural incision.

We next sought to validate boost-mediated augmentation of NIR fluorescence upon tumor exposure. Tumor views were obtained for 7 of 11 study subjects. An example case of an atypical meningioma (ICG 179) is presented

in Fig. 4. Marked enhancement in NIR fluorescence was observed as a result of excitation boost, elevating SBR from 1.7 ± 0.24 pre-boost to 2.1 ± 0.48 post-boost (Fig. 4a, middle and lower panels). Furthermore, ICG fluorescence was specifically confined to the tumor mass. Pre- and postoperative patient MRI images confirmed successful resection of the lesion (Fig. 4b).

Across all patients, boost excitation resulted in 35.45% mean improvement over pre-boost SBRs, and mean 1.36 ± 0.19 pre-boost and 1.81 ± 0.23 post-boost (Fig. 5a). The statistical significance of SBR increase attributable to excitation boost was supported by both two-tailed ratio paired *t* test ($p < 0.001$) and by Wilcoxon matched pairs signed rank test ($p < 0.001$). Additionally, excitation boost-mediated increase in SBR was observed across tumor, cortical, and dural views (Fig. 5b). This effect was consistently more pronounced under direct tumor visualization (44.28% increase in SBR, $p = 0.008$) than through dura and cortex, which are likely affected by the extent of excitation light and emission signal penetration through additional tissue layers.

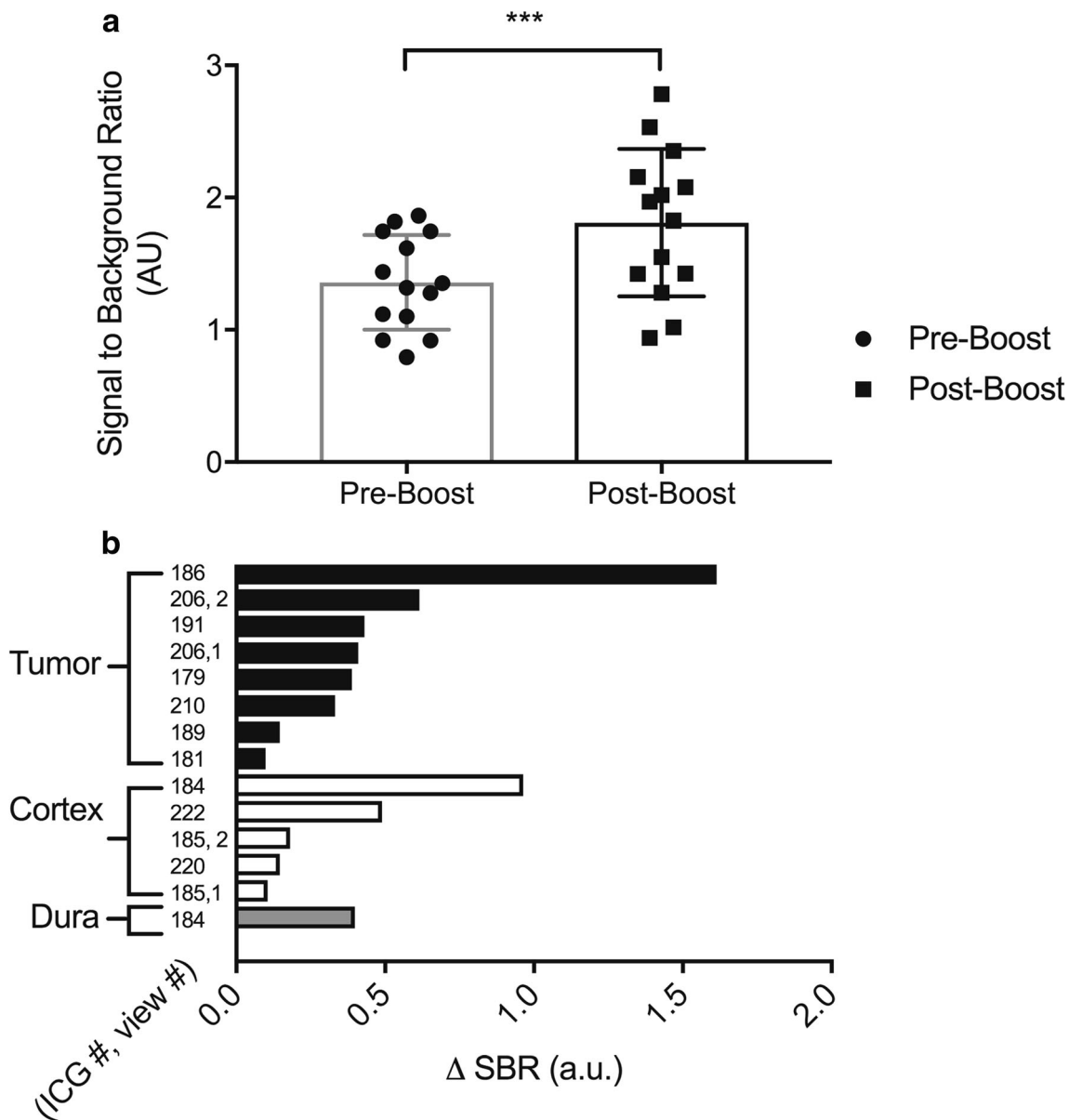


Fig. 5 Increase in mean signal to background ratio (SBR) for dura, cortex, and tumor view in all patients pre- and post-boost. **a** SBR (arbitrary units, AU) calculated across all patients ($n = 11$) and views ($n = 14$), including dura, cortex, and tumor, demonstrates 35.45% increase in mean SBR ($p < 0.001$) determined to be statistically

significant by Wilcoxon matched-pairs sign rank test. **b** Distribution of absolute change in SBR (Δ SBR) from pre-boost for all views obtained separated by tumor, cortex, or dura. Cases in which multiple tumor or cortex views were obtained for a given patient are specified by “view 1” and “view 2”

Collectively, these results suggest that the addition of narrow wavelength boost excitation to the fluorescence module of a standard neurosurgical microscope provides an effective means of augmenting NIR fluorescence intensity for intraoperative visualization of intracranial tumors.

Discussion

In this study, we applied a focused 805-nm laser excitation on top of an existing neurosurgical microscope fluorescence

module with the hypothesis that this technique, termed “boost excitation,” would improve detection of intraoperative NIR fluorescence. Our results indicate that application of high power, narrow-bandwidth excitation produced visible and quantifiable benefit to fluorescent image quality.

We recently compared intraoperative utility of the Leica FL800™ module to the VisionSense Iridium™, a dedicated commercial NIR imaging platform, with respect to NIR image quality and fluorescence sensitivity [1]. We demonstrated superior sensitivity of dedicated NIR-imaging platforms but noted that several factors restrict their intraoperative utility and

limit their widespread adoption. Neurosurgical microscopes therefore remain the preferred instrumentation for fluorescence-guided resections despite comparatively weaker NIR fluorescence sensitivity.

Using a delayed perfusion technique called Second Window ICG (SWIG), our group has expanded ICG NIR fluorescence from its prototypical application in cerebral angiography and demonstrated its capability for visualization of intracranial tumors [2, 10, 11]. Because the mechanism of SWIG relies on sustained retention of ICG following vascular perfusion, tumor ICG concentrations at the time of surgery are most likely lower than ICG concentrations in the vasculature immediately following bolus infusion. Therefore, SWIG requires intensified NIR excitation compared to vascular imaging.

Figure 6 a depicts a simplified emission scheme with a single peak at 805 nm corresponding to the optimal excitation wavelength of ICG in blood. During NIR fluorescence

visualization with the FL800™, exchange of Filter 1 for Filter 2 allows expanded passage (400–805 nm) of near-infrared wavelengths which supplies frequencies for ICG excitation. We propose that delivery of additional 805-nm light excites ICG to a greater magnitude and consequently increases fluorescence signal intensity (Fig. 6b). Second Window ICG is predicated on the notion that at the time of surgery, normal surrounding brain tissue contains essentially zero ICG and is therefore a constant. Signal to background pre- and post-boosts do not substantially increase background signal, disproportionately reflecting the increase in fluorescence emanating from tumor.

Several factors might influence interpretation of this study. First, boosts of tumor views were only obtained in a subset of patients (4/11) and was deferred for cases in which the operative angle or field of view was prohibitive [1]. Second, precise quantification of improvement in tumor fluorescence can be limited by tumor variability, and limited sample size

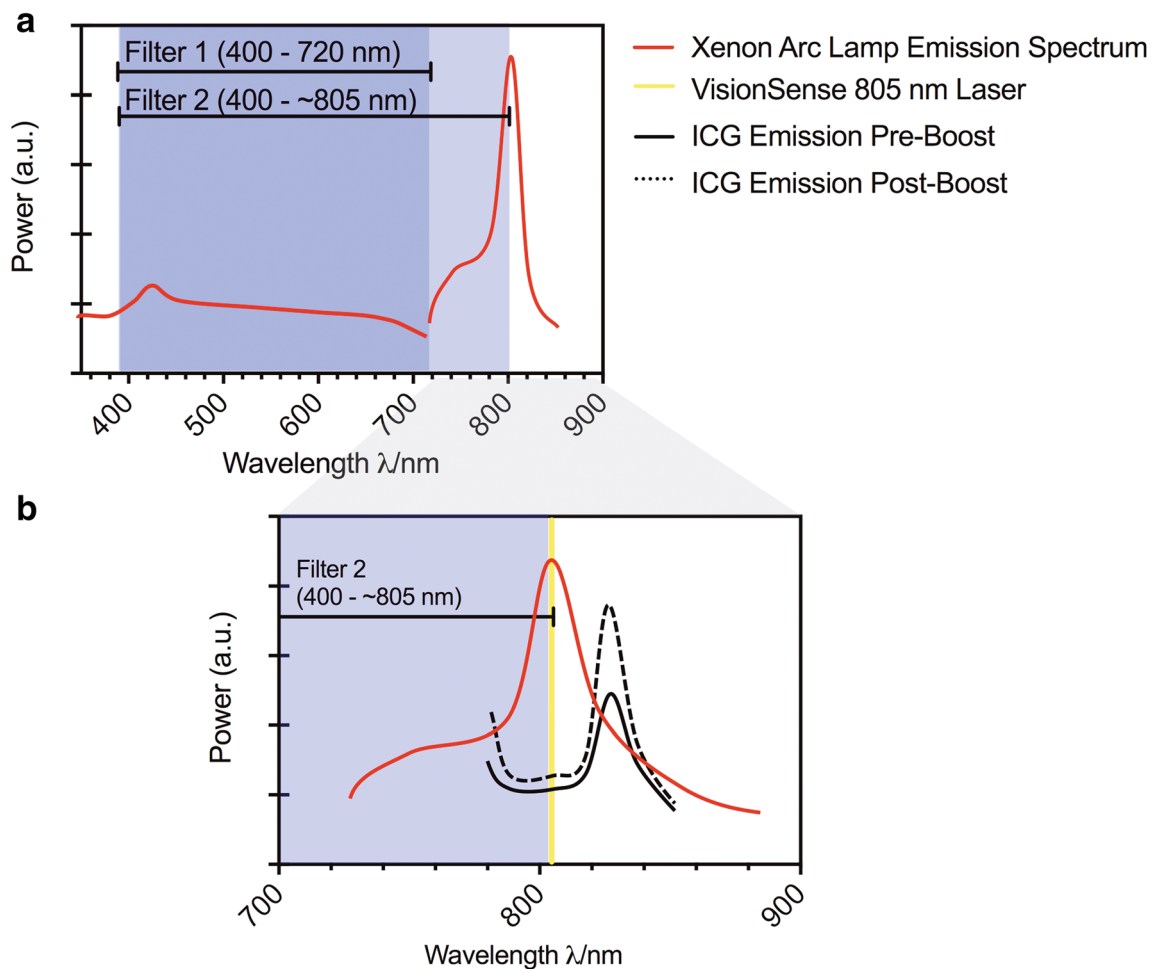


Fig. 6 Schema of boost excitation mechanism. **a** Illustration xenon broadband emission spectrum in the visible spectral range with complex emission profile in the near-infrared. The xenon light source for the Leica OH6 surgical microscope utilizes Filter 1 to block frequencies > 720 nm. The near-infrared fluorescence module FL800™

modifies this light source to allow selective transmission of frequencies in the 805-nm range (Filter 2) corresponding to peak excitation wavelength of ICG. **b** Magnified view of near-infrared spectrum illustrating postulated increase in ICG fluorescence resulting from addition of a focused 805-nm laser borrowed from the VisionSense Iridium Camera

precluded tumor specific analysis. One important point the authors wish to emphasize with respect to this limitation is that the boost technique is not intended to improve visualization of tumor margins, but rather to improve overall fluorescence intensity. We have previously described test characteristics of ICG for delineation of tumor margins [5]. In addition, boost excitation was only assessed in one neurosurgical microscope, limiting our ability to comment upon generalizability of this technique with respect to competitor microscopes. Equipment manufacturers may recognize constraints of existing modules but have particular reasons as to why a separate light source is not feasible in the clinical setting. Finally, the authors recognize that boost excitation only manipulates only the ICG excitation phase, which is one of many variables which determine final fluorescence output.

These limitations aside, the rapid development of targeted fluorophores incorporating near-infrared dyes—two examples IRDye 800CW conjugated to chlorotoxin, or TumorPaint™, and EGFR antibody cetuximab conjugated to IRDye800 for glioblastoma—suggest applicability of our findings beyond Second Window ICG [4, 8, 9]. Both underscore growing requirements for high power, focused excitation aimed at optimizing visualization of tumor fluorescence.

The ultimate aim of SWIG-guided tumor resections is to drive surgical decision-making. Towards this end, future microscope modules that project NIR fluorescence signals into microscope eyepieces will allow the integration of fluorescent view with the stereoscopic microscopic field-of-view. Our results provide the proof-of-principle evidence that a dedicated NIR light source would serve as a beneficial addition to existing neurosurgical microscope platforms; such modifications will allow more effective incorporation of SWIG into standard surgical workflow in resection of intracranial tumors.

Funding information Research reported in this publication was funded by the National Center for Advancing Translational Sciences of the National Institutes of Health under Award Number UL1TR001878. The content is solely the responsibility of the authors and does not necessarily represent the official views of the NIH. Additional financial support was received from the Institute for Translational Medicine and Therapeutics of the University of Pennsylvania. Funding sources had no role in the design or conduct of this research.

Compliance with ethical standards

Conflict of interest The authors declare that they have no conflict of interest.

Ethical approval All procedures performed in this study involving human participants were in accordance with the ethical standards of the institutional research committee of the Hospital of the University of

Pennsylvania and with the 1964 Helsinki declaration and its later amendments or comparable ethical standards.

Informed consent Informed consent was obtained from all individual participants included in the study.

References

1. Cho SS, Zeh R, Pierce J et al (2018) Comparison of near-infrared imaging camera systems for intracranial tumor detection. *Mol Imaging Biol* 20(2):213–220. <https://doi.org/10.1007/s11307-017-1107-5>
2. DSouza AV, Lin H, Henderson E et al (2016) Review of fluorescence guided surgery systems: identification of key performance capabilities beyond indocyanine green imaging. *J Biomed Opt* 21(8):080901. <https://doi.org/10.1117/1.JBO.21.8.080901>
3. Jiang JX, Keating JJ, Jesus E et al (2015) Optimization of the enhanced permeability and retention effect for near-infrared imaging of solid tumors with indocyanine green. *Am J Nucl Med Mol Imaging* 5(4):390–400 Available at: <http://www.ncbi.nlm.nih.gov/pubmed/26269776> (Accessed: 20 Aug 2018)
4. Kovar JL, Curtis E, Othman S et al (2013) Characterization of IRDye 800CW chlorotoxin as a targeting agent for brain tumors. *Anal Biochem* 440(2):212–219. <https://doi.org/10.1016/j.ab.2013.05.013>
5. Lee JYK, Thawani JP, Pierce J et al (2016) Intraoperative near-infrared optical imaging can localize gadolinium-enhancing gliomas during surgery. *Neurosurgery* 79(6):856–871. <https://doi.org/10.1227/NEU.0000000000001450>
6. Lee JYK, Pierce JT, Zeh R et al (2017) Intraoperative near-infrared optical contrast can localize brain metastases. *World Neurosurgery* 106:120–130. <https://doi.org/10.1016/j.wneu.2017.06.128>
7. Lee JYK, Pierce JT, Thawani J et al (2018) Near-infrared fluorescence image-guided surgery for intracranial meningioma. *J Neurosurg* 128(2):380–390. <https://doi.org/10.3171/2016.10.JNS161636>
8. Miller SE, Tummers W, Theraphongphom N et al (2018) First-in-human intraoperative near-infrared fluorescence imaging of glioblastoma using cetuximab-IRDye800. *J Neuro-Oncol* 139(1):135–143. <https://doi.org/10.1007/s11060-018-2854-0>
9. Warram, J. M., de Boer E., Korb M. et al. (2015) ‘Fluorescence-guided resection of experimental malignant glioma using cetuximab-IRDye 800CW’, *Br J Neurosurg.* 29(6), pp. 850–858. doi: <https://doi.org/10.3109/02688697.2015.1056090>
10. Zeh R, Sheikh S, Xia L et al (2017) The second window ICG technique demonstrates a broad plateau period for near infrared fluorescence tumor contrast in glioblastoma. *PLOS ONE* Edited by M Bogyo 12(7):e0182034. <https://doi.org/10.1371/journal.pone.0182034>
11. Zhang DY, Singhal S, Lee JYK (2018) Optical principles of fluorescence-guided brain tumor surgery: a practical primer for the neurosurgeon. *Neurosurgery.* <https://doi.org/10.1093/neuros/nyy315>

Publisher’s note Springer Nature remains neutral with regard to jurisdictional claims in published maps and institutional affiliations.